

Why magnetism in $\text{CeO}_{1-x}\text{F}_x\text{FeAs}$ and $\text{LaO}_{1-x}\text{F}_x\text{FeAs}$ is different

S. Sharma^{1,2,3,*}, S. Shallcross⁴, J. K. Dewhurst^{1,2,3}, A. Sanna^{2,6}, C. Bersier^{1,2,3}, H. Glawe^{2,3}, and E. K. U. Gross^{2,3}

¹ Fritz Haber Institute of the Max Planck Society, Faradayweg 4-6, D-14195 Berlin, Germany.

² Institut für Theoretische Physik, Freie Universität Berlin, Arnimallee 14, D-14195 Berlin, Germany

³ European Theoretical Spectroscopy Facility (ETSF) and

⁴ Lehrstuhl für Theoretische Festkörperphysik, Staudstr. 7-B2, 91058 Erlangen, Germany.

Using state-of-the-art first-principles calculations we study the magnetic behaviour of CeOFeAs . We find the Ce layer moments oriented perpendicular to those of the Fe layers. An analysis of incommensurate magnetic structures reveals that the Ce-Ce magnetic coupling is rather weak with, however, a strong Fe-Ce coupling. Comparison of the origin of the tetragonal to orthorhombic structural distortion in CeOFeAs and LaOFeAs show marked differences; in CeOFeAs the distortion is stabilized by a lowering of spectral weight at the Fermi level, while in LaOFeAs by a reduction in magnetic frustration. Finally, we investigate the impact of electron doping upon CeOFeAs and show that while the ground state Fe moment remains largely unchanged by doping, the stability of magnetic order goes to zero at a doping that corresponds well to the vanishing of the Néel temperature.

PACS numbers: 74.25.Jb, 67.30.hj, 75.30.Fv, 75.25.tz, 74.25.Kc

The recently discovered [1, 2] family of FeAs based compounds that, upon electron doping, become superconducting with transition temperatures up to 55K, are attracting a lot of interest. Structurally these materials ROFeAs ($\text{R}=\text{La, Ce, Pr, Nd, Sm}$) are very similar in that they are formed from FeAs layers separated by rare earth or lanthanide oxide layers. In striking contrast to the well known cuprates, these materials are weakly magnetic metals, leading to the possibility of large spin fluctuation effects [3, 4]. In particular, at the onset of superconductivity the moment on the Fe atoms vanishes, and a key question concerns the possible role of such spin fluctuations in the superconducting transition [3, 4].

Despite the diverse set of rare earth and lanthanide atoms involved in these materials, physically they share many similarities. In particular, (i) at temperatures around $\sim 150\text{K}$ a structural phase transition from tetragonal to orthorhombic crystal symmetry occurs and, (ii) this is then closely followed by a magnetic phase transition to a spin order anti-ferromagnetic (AFM) in nature, (iii) upon doping with Fluorine the AFM order is suppressed and superconductivity appears. Furthermore, calculations reveal that (iv) the non-magnetic Fermi surfaces are all strongly nested [3, 5, 6], and (v) that the moment of the Fe atoms depends critically upon the separation of the Fe layer from the adjacent As layer [5, 7, 8].

Given the diversity of constituents involved in this class of materials, such uniformity of behaviour appears, at first sight, somewhat surprising. The question then arises if the underlying physical mechanisms behind such phenomenon as the structural distortion or doping behaviour are also the same. In the present work we investigate this by analyzing the properties of CeOFeAs as compared to the well studied LaOFeAs . The choice of these two materials is motivated by the fact that amongst the rare earth and lanthanide oxypnictides they show rela-

tively large differences for two key physical properties; (i) the low temperature moment of the Fe atom, $0.35\mu_B$ in LaOFeAs is the lowest while in CeOFeAs ($0.94\mu_B$) is the highest amongst all oxypnictides [9, 10, 11, 12], and (ii) the superconducting transition temperature also differs strongly; 26 K in LaOFeAs [1, 13] and 45 K in CeOFeAs [14, 15, 16].

Remarkably, we find that the mechanism behind the structural phase transition in CeOFeAs and LaOFeAs is quite different; the former case being driven, essentially, by the one electron kinetic energy i.e. Fermi surface effects, while the latter is driven by magnetic frustration [8, 17]. In addition, the behaviour upon electron doping is substantially different. We find that for $\text{CeO}_{(1-x)}\text{F}_x\text{FeAs}$ the moment is *almost unchanged* upon electron doping (a reduction of 3% for $x = 0.10$), whereas calculations of $\text{LaO}_{(1-x)}\text{F}_x\text{FeAs}$ have revealed a strong suppression of the moment (90% at $x = 0.10$). This may be reconciled with the vanishing of the Néel temperature at $x = 0.06$ by the fact that the magnetic order becomes *meta-stable* near this doping.

In the present work all calculations are performed using the state-of-the-art full-potential linearized augmented plane wave (FP-LAPW) method [18], implemented within the Elk code [19]. To obtain the Pauli spinor states, the Hamiltonian containing only the scalar potential is diagonalized in the LAPW basis: this is the first-variational step. The scalar states thus obtained are then used as a basis to set up a second-variational Hamiltonian with spinor degrees of freedom [18]. This is more efficient than simply using spinor LAPW functions, but care must be taken to ensure that there is a sufficient number of first-variational eigenstates for convergence of the second-variational problem. We use a shifted \mathbf{k} mesh of $10 \times 10 \times 6$, and 260 states per \mathbf{k} -point which ensures convergence of the second variational step as well as the

convergence with respect to the \mathbf{k} -points. All the experimental lattice parameters from Ref. 14 have been used.

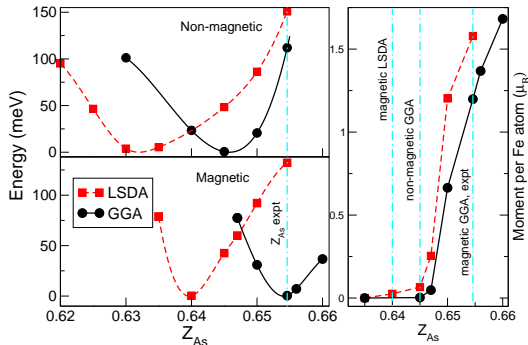


FIG. 1: (color online) Top-left panel: energy (in meV) per formula unit as a function of position of the As atom calculated using LDA and GGA. Bottom-left panel: same as upper panel but the calculation is spin-polarized. Right-hand panel shows the moment per Fe atom (in μ_B) calculated using LSDA and GGA.

We first consider the undistorted undoped ground state of CeOFeAs. One of the most striking aspects of the theoretically intensively studied compound LaOFeAs has been the spread of results for magnetic properties, attributed to both an unusual sensitivity to the approximation to exchange-correlation, and a sensitive dependence upon the separation of the Fe and As layers, z_{As} [5, 7, 8]. This latter behaviour is also found in the case of CeOFeAs[20], however in contrast to LaOFeAs a spin polarized generalized gradient approximation (GGA)[21] calculation yields an optimized z_{As} in near perfect agreement with experiment, see Fig. 1.

Given this choice of z_{As} we now determine the ground state magnetic structure using, in addition to the GGA functional, the local spin density approximation (LSDA)[22] and LSDA+U[23] functionals (for the latter we use $U = 6$ eV and $J = 1$ eV for the Ce atom). Considering first only collinear structures, we find that the Fe layer adopts the stripe AFM structure found in all the oxypnictides, with the magnetic moments of the Ce layer perpendicular to those of the Fe layer. The Fe (Ce) moments are found to be $1.58\mu_B$ ($0.56\mu_B$), $1.52\mu_B$ ($0.92\mu_B$), and $1.30\mu_B$ ($0.54\mu_B$) for the LSDA, LSDA+U, and GGA functionals respectively, with the corresponding experimental values $0.94\mu_B$ for Fe and $0.83\mu_B$ for Ce. The agreement with experiment for the Fe moment is thus rather poor for all functionals considered. This may be attributed to the exceptionally sensitive dependence of the Fe moment on z_{As} , see Fig. 1, which for CeOFeAs is even more pronounced than in LaOFeAs. Interestingly,

as indicated in experiments[14] we find that the Ce and Fe moments are strongly coupled; a small change (1%) of the Ce moment (performed with a fixed spin calculation), leads to a large change (3%) in the Fe moment.

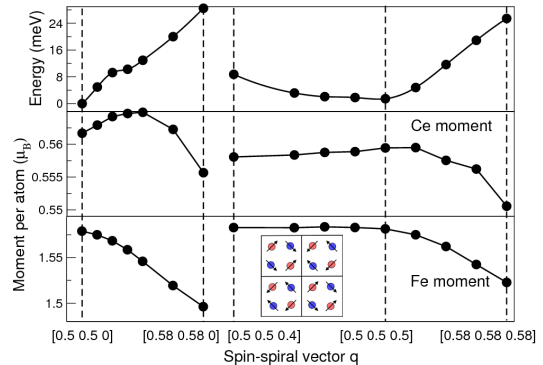


FIG. 2: (color online) Top panel shows the energy (in meV per formula unit) and the middle and bottom panels show the magnetic moment (in μ_B) per Ce and Fe atom respectively. All quantities are plotted as a function of the spin-spiral q -vector. The inset is a schematic of the spin configuration of the Fe and Ce atoms.

In order to study the possible incommensurate spin structure we have calculated the total energy as a function of the spin-spiral vector \mathbf{q} , for various directions in the Brillouin zone (BZ). For the in plane spin spirals (going in the direction $[0.5, 0.5, 0]$ to $[1, 1, 0]$) we find a clear sharp minimum at the commensurate \mathbf{q} vector of $[0.5, 0.5, 0]$, equivalent to stripe AFM spin configuration (top panel Fig. 2). Interestingly, however, we find that the various spin configurations are almost degenerate in the direction $[0.5, 0.5, 0.4]$ to $[0.5, 0.5, 0.5]$. This is indicative of weak inter-plane Ce-Ce and Fe-Fe coupling; this finding is concomitant with experimental results of Zhao *et al.*[14]

Turning now to the spin spiral moments (lower two panels Fig. 2), we find that the moment remains almost unchanged upon changing the magnetic structure away from the stripe AFM spin configuration. This is in striking contrast to LaOFeAs, which remains spin polarized [8, 24, 25] only in a small region about the M point ($[0.5, 0.5, 0]$), with the moment vanishing elsewhere in the BZ. Since for CeOFeAs the moment on the Fe atoms changes only slightly - 5.2% - upon moving across the BZ hence the role of spin fluctuations could be rather different in these two materials.

This difference may be understood as a consequence of the nature of the various *inter-plane* and *intra-plane* magnetic couplings in this material. In particular, the intra-plane coupling of the Ce atoms is very weak - we find the energy difference between FM and AFM ordered in-plane Ce moments to be almost degenerate with, ad-

ditionally, the magnitude of the Ce moments unchanged by this choice of FM or AFM order. Thus the nature of the Ce-Ce interaction results in the Ce moment remaining unchanged by a spin wave configuration; this in turn acts to preserve the Fe moment due to the strong inter-plane Fe-Ce coupling.

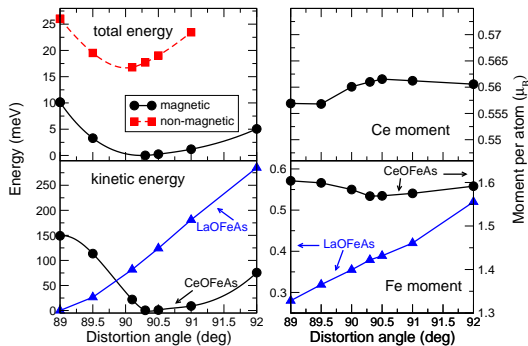


FIG. 3: (color online) Top-left panel shows the total energy and bottom-left panel the one-electron kinetic energy (in meV) per formula unit. The right panel shows the moment per Ce (top) and Fe (bottom) atom (in μ_B) as a function of distortion angle (in degrees).

As with all the oxypnictides, CeOFeAs undergoes a structural phase transition from tetragonal to orthorhombic crystal symmetry[14], which in this compound occurs at 160K. In order to determine the physical reason behind this transition we have performed *ab-initio* LSDA calculations. As may be seen in Fig. 3 the non-magnetic compound does not show any crystal distortion, but upon performing spin polarized calculations one finds a minimum in energy at a distortion angle of 90.30° . The difference in energy between the non-magnetic undistorted and magnetic distorted materials is 17meV (197 K), which is comparable to the experimental critical temperature of 160K. Thus both the distortion and critical temperatures are very similar to those found in LaOFeAs however, as we will now show, the underlying mechanism of the transition is entirely different.

In the case of LaOFeAs the crystal distortion could be rationalized as being driven by an increase in moment upon distortion[8], due to a lowering of magnetic frustration in the distorted lattice[8, 17]. On the other hand, the moment of both Fe and Ce atoms remains essentially unchanged in CeOFeAs upon distortion, see right hand panels of Fig. 3, thus ruling out such a mechanism for this compound. However, the one-electron kinetic energy of CeOFeAs shows a clear minimum at 90.30° while, in dramatic contrast, the LaOFeAs one electron kinetic energy monotonically increases as a function of distortion angle. Thus the structural distortion in CeOFeAs is driven by an electronic structure mechanism, in contrast

to the frustration driven mechanism of LaOFeAs. In this regard in Fig. 4 are shown the non-magnetic as well as magnetic (AFM stripe phase) density of states (DOS) for the undistorted and distorted lattices. One feature com-

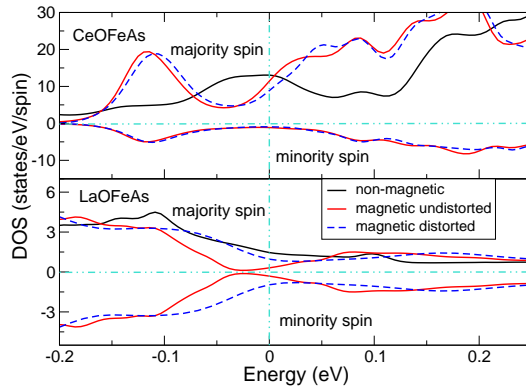


FIG. 4: (color online) Density of states calculated using the LSDA for undistorted non-magnetic, undistorted magnetic and distorted magnetic structures for CeOFeAs and LaOFeAs. Stripe anti-ferromagnetic order was used for the magnetic calculations.

mon to both compounds is that, as one would expect, spin polarization results in a large shift of spectral weight away from the Fermi level. Turning to the impact of distortion one observes a striking difference: in LaOFeAs there is a substantial *increase* in spectral weight at the Fermi level[17, 26] while, in contrast, in CeOFeAs spectral weight is moved away from the Fermi level. Thus in this latter case the redistribution of spectral weight drives the transition, while for LaOFeAs the opposite is the case. Clearly, therefore, although both the distortion angle and transition temperatures are very similar in these two oxypnictides, the origin of the structural phase transitions is very different. At this point it is also worth mentioning that heat capacity measurements of McGuire *et al.* showed that this decrease of the DOS at the Fermi level in CeOFeAs on distortion is consistent with the Seebeck coefficient measurements[27].

The most important property of the iron oxypnictides is the occurrence of a superconducting phase transition at a critical electron doping[14, 15, 28, 29]. An interesting difference between the temperature-doping phase diagrams of $\text{CeO}_{1-x}\text{F}_x\text{FeAs}$ and $\text{LaO}_{1-x}\text{F}_x\text{FeAs}$ is that, for the former case, the Néel temperature of the magnetic phase goes continuously to zero[14] as critical doping is approached ($x_c = 0.06$), while in $\text{LaO}_{1-x}\text{F}_x\text{FeAs}$ one instead finds a sharp drop[9, 30, 31] in the Néel temperature at a critical doping of $x_c = 0.045$ (see right hand panel Fig. 5). Concomitantly, low temperature

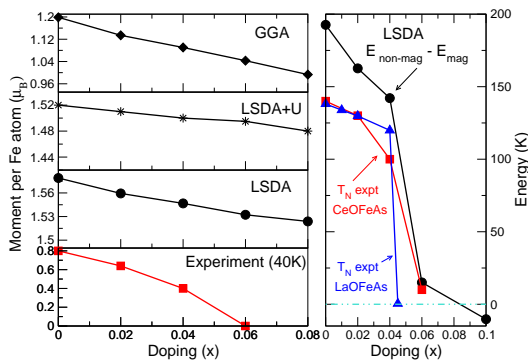


FIG. 5: (color online) Left panel: moment per Fe atom (in μ_B) as a function of doping calculated using the LSDA, LSDA+U and GGA. The right panel: shows the difference between the magnetic and the non-magnetic total energy (in K) calculated using the LSDA. The experimental data for $\text{CeO}_{1-x}\text{F}_x\text{FeAs}$ are taken from Ref. 14 and for $\text{LaO}_{1-x}\text{F}_x\text{FeAs}$ from Ref. 9

measurements of the magnetic order of the Fe layer in $\text{CeO}_{1-x}\text{F}_x\text{FeAs}$ show that it is entirely lost before x_c (left panel Fig. 5). An important question for understanding the role of magnetism in the superconducting transition is then whether it is the moment of the Fe atoms that vanishes, or whether it is simply the stripe AFM order that vanishes.

To investigate this issue we calculate $\text{CeO}_{1-x}\text{F}_x\text{FeAs}$ by deploying the virtual crystal approximation (VCA). Although the VCA neglects much of the physics of disorder, it has been shown recently[32] to provide a surprisingly accurate account of magnetism and Fermiology in $\text{LaO}_{1-x}\text{F}_x\text{FeAs}$. In order to determine the impact of the approximation to the xc functional, calculations were performed using the LSDA, LSDA+U, and GGA functionals.

Amongst the undoped Fe oxypnictides the Fe moment is largest in CeOFeAs and smallest in LaOFeAs, and it is therefore surprising that in the latter compound the magnetic phase appears more stable for $x < x_c$. Indeed, calculations of the Fe moment in $\text{CeO}_{1-x}\text{F}_x\text{FeAs}$ (left panel Fig. 5) show that, in apparent contradiction to the experimental data, there is *almost no change* upon doping. However, if we consider the magnetization energy, i.e. the quantity $E_{\text{non-mag}} - E_{\text{mag}}$ (right panel Fig. 5), this falls sharply at exactly the critical doping $x_c = 0.06$. Thus it is the *stability* of the magnetic order which is reduced upon doping, not the actual Fe moment. This sudden reduction of stability, which is not found in $\text{LaO}_{1-x}\text{F}_x\text{FeAs}$, is behind the differing forms of the Néel temperature phase boundary.

In the case of LaOFeAs calculations have shown[8] that, upon doping, the distortion angle changes from an undoped value of $\theta = 90.27^\circ$ to $\theta = 89.85^\circ$; addition-

ally, there is the appearance of incommensurate magnetic phases. We have investigated if such phases appear in the doping phase diagram of $\text{CeO}_{1-x}\text{F}_x\text{FeAs}$ and find that (i) the distortion angle is unchanged upon doping ($0 \leq x \leq 0.06$) and (ii) the ground state magnetic structure remains stripe AFM.

To conclude, we have performed a comparative study of the two oxypnictides $\text{CeO}_{1-x}\text{F}_x\text{FeAs}$ and $\text{LaO}_{1-x}\text{F}_x\text{FeAs}$. Although many common features, e.g. a similar non-magnetic Fermi surface, may be found in the iron oxypnictides we have shown here that profound differences also exist. In particular we find that the structural distortion in CeOFeAs is driven by one electron kinetic energy (i.e. electronic structure effect), in contrast to LaOFeAs where a lowering of magnetic frustration has been identified as the mechanism. Furthermore, the behaviour under electron doping differs markedly between the two materials; in $\text{CeO}_{1-x}\text{F}_x\text{FeAs}$ we find that while the ground state moment is essentially unchanged with doping, the *stability* of the moment is sharply reduced. Finally, we have - via calculations of incommensurate spin spiral structures - carefully investigated the various magnetic couplings of the constituents of CeOFeAs; we find that the Ce atoms are only weakly coupled to each other, while the Fe atoms are much more strongly coupled to each other as well as to the Ce.

* Electronic address: sangeeta.sharma@physik.fu-berlin.de

- [1] Y. Kamihara et al., J. Am. Chem. Soc. **130**, 3296 (2008).
- [2] Z.-A. Ren et al., Phys. Rev. B **78**, 092505 (2008).
- [3] I. I. Mazin et al., Phys. Rev. Lett. **101**, 057003 (2008).
- [4] I. I. Mazin and M. D. Johannes, Nature **5**, 141 (2009).
- [5] Z. P. Yin et al., Phys. Rev. Lett. **101**, 047001 (2008).
- [6] L. Pourovskii et al., Europhys. Lett. **84**, 37006 (2009).
- [7] I. I. Mazin et al., Phys. Rev. B **78**, 085104 (2008).
- [8] S. Sharma et al. (2008), arXiv:0810.4278.
- [9] H. Luetkens et al., Nat. Mater. (2009), 10.1038/nmat2397.
- [10] T. Nomura et al., Supercond. Sci. Tech. **21**, 125028 (2008).
- [11] H.-H. Klauss et al., Phys. Rev. Lett. **101**, 077005 (2008).
- [12] C. de la Cruz et al., Nature **453**, 899 (2008).
- [13] H.-H. Wen et al., Phys. Rev. Lett. **82**, 17009 (2008).
- [14] J. Zhao et al., Nature Mat. **7**, 953 (2008).
- [15] G. F. Chen et al., Phys. Rev. Lett. **100**, 247002 (2008).
- [16] D. A. Zocco et al., Physica C **468**, 2229 (2008).
- [17] T. Yildirim, Phys. Rev. Lett. **101**, 057010 (2008).
- [18] D. J. Singh and L. Nordström, Planewaves Pseudopotentials and the LAPW Method, pringer, New York (2006).
- [19] J. K. Dewhurst et al. (2004), URL <http://elk.sourceforge.net>.
- [20] H. M. Alyahyaei and R. A. Jishi, Phys. Rev. B **79**, 064516 (2009).
- [21] J. Perdew et al., Phys. Rev. Lett. **77**, 3865 (1996).
- [22] J. Perdew and Wang, Phys. Rev. B **45**, 13244 (1992).
- [23] A. I. Liechtenstein et al., Phys. Rev. B **52**, R5467 (1995).
- [24] A. N. Yaresko et al. (2008), arXiv:0810.4469.

- [25] J. Lorenzana et al., Phys. Rev. Lett. **101**, 186402 (2008).
- [26] J. Dong et al., Europhys. Lett. **83**, 27006 (2008).
- [27] M. A. McGuire et al. (2008), arXiv:0811.0589.
- [28] F. Bondino et al., Phys. Rev. Lett. **101**, 267001 (2008).
- [29] S. Chi et al., Phys. Rev. Lett. **101**, 217002 (2008).
- [30] Q. Huang et al., Phys. Rev. B **78**, 054529 (2008).
- [31] D. R. Garcia et al., Phys. Rev. B **78**, 245119 (2008).
- [32] P. Larson and S. Satpathy, Phys. Rev. B **79**, 054502 (2009).